

## Study of the coupling of interlayers in compositionally modulated FeSi/Si amorphous films by conversion electron Mossbauer spectroscopy

This article has been downloaded from IOPscience. Please scroll down to see the full text article.

1991 J. Phys.: Condens. Matter 3 7139

(<http://iopscience.iop.org/0953-8984/3/37/005>)

View [the table of contents for this issue](#), or go to the [journal homepage](#) for more

Download details:

IP Address: 171.66.16.147

The article was downloaded on 11/05/2010 at 12:33

Please note that [terms and conditions apply](#).

# Study of the coupling of interlayers in compositionally modulated FeSi/Si amorphous films by conversion electron Mössbauer spectroscopy

X D Ma, Y H Liu and L M Mei

Department of Physics, Shandong University, Jinan, Shandong, People's Republic of China

Received 4 January 1991, in final form 14 March 1991

**Abstract.** Compositionally modulated FeSi/Si amorphous films with a fixed FeSi layer thickness and different Si layer thicknesses have been studied by  $^{57}\text{Fe}$  conversion electron Mössbauer spectroscopy at room temperature. The results showed that, with decreasing Si layer thickness, the hyperfine fields of samples increased and the thickness of the interface dead layers arising from the atomic interdiffusion effect decreased. These are due to the coupling effect between the magnetic layers. When the Si layers are thinner than 8.8 Å, the direction of the magnetization is out of the film plane.

## 1. Introduction

Recently, the study of compositionally modulated films (CMFs) has attracted much attention because these films possibly exhibit new magnetic properties. In particular, amorphous CMFs have no serious crystal-lattice-matching problems at the interfaces, and it is easy to obtain better modulated structures. Amorphous FeSi/Si CMFs with a fixed FeSi layer thickness and different Si layer thicknesses have been prepared by RF sputtering, and a good modulated structure has been obtained.

In the FeSi/Si CMF, atomic interdiffusion between magnetic and non-magnetic layers would inevitably exist because of the ion implantation effect during the sputtering process and the solubility of Fe and Si. This results in the formation of paramagnetic dead layers at the interfaces. These dead layers directly affected the magnetic properties of the CMF [1, 2]. When the non-magnetic layers are thin enough, magnetic coupling between magnetic layers is induced and strengthened with decreasing non-magnetic layer thickness. This will influence the dead layers and the internal fields of samples. In this paper,  $^{57}\text{Fe}$  conversion electron Mössbauer spectroscopy (CEMS) has been used to study the coupling effects of interlayers for the FeSi/Si CMF.

## 2. Experimental details

The amorphous FeSi/Si CMFs were prepared by an RF sputtering system with two targets. During the process of sample preparation, the base pressure was about  $1 \times 10^{-6}$  Torr, and then 99.999% pure Ar gas was introduced. The Ar gas pressure was kept at

$5 \times 10^{-3}$  Torr. The RF input power was about 180 W. The substrates were glass slides of 0.2 mm thickness and were cooled by water. The deposition rates of FeSi and Si were  $0.85 \text{ \AA s}^{-1}$  and  $0.88 \text{ \AA s}^{-1}$ , respectively. By alternatively controlling the sputtering time of FeSi and Si, a series of samples was obtained. The thickness of the FeSi layers was fixed at  $17 \text{ \AA}$ , while the thickness of the Si layers varied from 8.8 to  $101 \text{ \AA}$ . The total number of bilayers was 40 for all samples. The reason for choosing the thickness of the FeSi layers as  $17 \text{ \AA}$  is as follows: the study on the FeSi/Si CMFs with different FeSi layer thicknesses and fixed Si layer thickness at  $53 \text{ \AA}$  showed that, when the FeSi layer thickness is  $17 \text{ \AA}$  or thinner, the samples showed small magnetic hysteresis loops and had a lower Curie temperature and lower saturation magnetization. These are some characteristics of two-dimensional magnetism [3, 4]. When the thickness of the Si layers is varied, the influence of the coupling of interlayers on the magnetic properties of the FeSi/Si CMF would be reflected more distinctly. Single FeSi films were also prepared for comparison. The composition of FeSi films determined by the electron microprobe analysis was  $\text{Fe}_{80.5}\text{Si}_{19.5}$ . This is the lower limit of the composition where the amorphous feature is observed [5]. No crystalline peak was observed for single FeSi films from x-ray diffraction measurement.

The structural analysis of samples was made by using a standard x-ray diffractometer with  $\text{Cu K}\alpha$  radiation. Large-angle x-ray diffraction showed that all samples were amorphous. Bragg peaks due to the modulated structure were observed in the small-angle region for all samples. Four orders of diffraction peaks can be seen mostly. This indicated that all samples have good modulated structures. The modulated wavelengths of samples calculated using the Bragg diffraction law were in good agreement with the design values according to the deposition rates and the deposition time of FeSi and Si. The error was within 5%.

Conversion electron Mössbauer spectra of samples were recorded at room temperature using a gas flow ( $\text{CH}_3\text{COCH}_3$ ) proportional counter, a 5 mCi  $^{57}\text{Co}$ -Rh source (in the constant-acceleration mode), and a 1024-channel multichannel analyser. The spectrometer was calibrated with a standard  $\alpha$ -Fe foil.

### 3. Results and discussion

Figure 1 shows the Mössbauer spectra of FeSi/Si CMF samples with different thicknesses of the Si layers and a single FeSi film. For the FeSi/Si CMFs, the spectra can be roughly divided into two subspectra: one is a ferromagnetic sextet spectrum which originated from the ferromagnetic part in FeSi layers. Since the samples were amorphous, the lines are broadened. The other is a paramagnetic spectrum originating from the non-magnetic part at the interfaces, i.e. the dead layers. The spectra were fitted with the above two subspectra using Meisel's [6] method on a PDP 11/34 computer system. The fitted curves are shown as the full curves in figure 1. The data of the Mössbauer spectra are listed in table 1.

As shown in table 1, with decreasing thickness  $d_s$  of the Si layers, the hyperfine field  $H_f$  of the sample increases, while the percentage  $\alpha_p$  of paramagnetic component in the whole spectrum decreases and so does the thickness  $d_p$  of the dead layers which is defined as  $d_m\alpha_p$ . Here  $d_m$  is the thickness of the FeSi layers; in our case,  $d_m = 17 \text{ \AA}$ . The parameters of the paramagnetic subspectrum (an isomer shift (IS) of about  $0.22 \text{ mm s}^{-1}$  (with respect to  $\alpha$ -Fe), the quadrupole splitting (QS) of about  $0.65 \text{ mm s}^{-1}$  and the linewidth (LW) of about  $0.35 \text{ mm s}^{-1}$ ) are independent of the Si layer thicknesses.

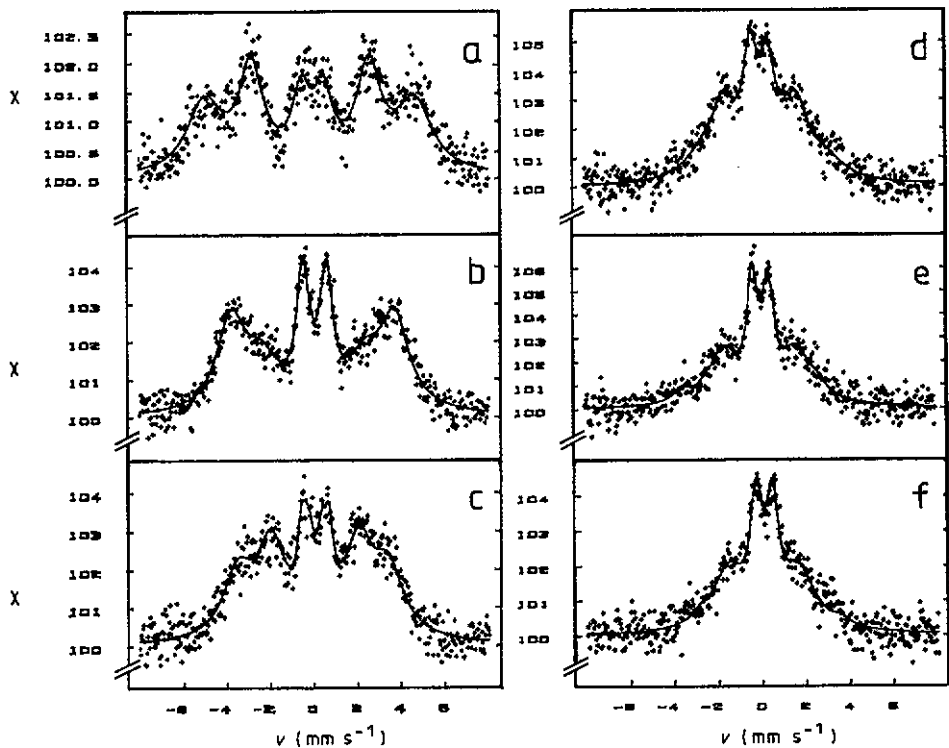


**Figure 1.** Conversion electron Mössbauer spectra at room temperature for a single FeSi film and FeSi/Si CMFs: (a) the single FeSi film with a thickness of 1370 Å; (b) FeSi (17 Å)/Si (8.8 Å); (c) FeSi (17 Å)/Si (13.2 Å); (d) FeSi (17 Å)/Si (26.4 Å); (e) FeSi (17 Å)/Si (53 Å); (f) FeSi (17 Å)/Si (101 Å). The full curves are the fitted curves.

**Table 1.** CEMS data of the amorphous FeSi/Si CMF.  $d_s$  is the thickness of the Si layers;  $H_f$  is the hyperfine field of samples (assume that  $H_f = 330$  kOe for  $\alpha$ -Fe),  $\Gamma_{16}$  is the linewidth of the first or sixth line and  $\delta$  is the isomer shift of the ferromagnetic subspectrum;  $is$ ,  $qs$  and  $lw$  are the isomer shift, quadrupole splitting and linewidth of the paramagnetic subspectrum, respectively;  $\alpha_p$  is the percentage of the paramagnetic component in the whole spectra;  $d_p$  is the thickness of the dead layers.

| Spectrum                 | Ferromagnetic component |                |  |                                     | Paramagnetic component          |                               |                               |                   | $d_p$<br>(Å) |
|--------------------------|-------------------------|----------------|--|-------------------------------------|---------------------------------|-------------------------------|-------------------------------|-------------------|--------------|
|                          | $d_s$<br>(Å)            | $H_f$<br>(kOe) | $\Gamma_{16}$<br>(mm s <sup>-1</sup> ) | $\delta^a$<br>(mm s <sup>-1</sup> ) | $is^a$<br>(mm s <sup>-1</sup> ) | $qs$<br>(mm s <sup>-1</sup> ) | $lw$<br>(mm s <sup>-1</sup> ) | $\alpha_p$<br>(%) |              |
| Figure 1(a) <sup>b</sup> | —                       | 289.69         | 0.98                                   | 0.07                                | —                               | —                             | —                             | —                 | —            |
| Figure 1(b)              | 8.8                     | 225.87         | 0.80                                   | 0.17                                | 0.22                            | 0.65                          | 0.35                          | 4.06              | 0.69         |
| Figure 1(c)              | 13.2                    | 208.22         | 0.82                                   | 0.19                                | 0.24                            | 0.63                          | 0.32                          | 12.39             | 2.11         |
| Figure 1(d)              | 26.4                    | 195.26         | 0.84                                   | 0.22                                | 0.21                            | 0.72                          | 0.36                          | 16.80             | 2.86         |
| Figure 1(e)              | 53                      | 192.30         | 0.87                                   | 0.23                                | 0.21                            | 0.68                          | 0.31                          | 18.01             | 3.06         |
| Figure 1(f)              | 101                     | 190.82         | 0.85                                   | 0.23                                | 0.22                            | 0.62                          | 0.34                          | 18.50             | 3.14         |

<sup>a</sup> With respect to  $\alpha$ -Fe.

<sup>b</sup> Single FeSi film with a thickness of 1370 Å.

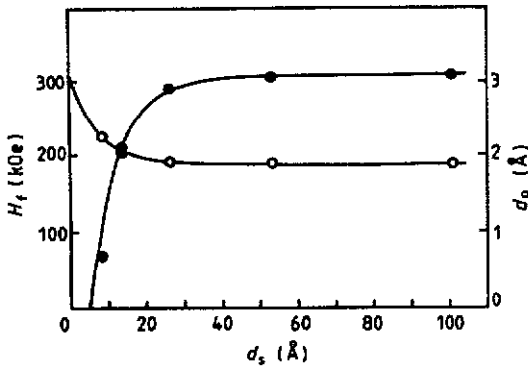


Figure 2. The hyperfine field  $H_f$  (○) and the thickness  $d_p$  (●) of the dead layers as functions of the thickness  $d_s$  of the Si layers. The full curves for  $H_f$  and  $d_p$  are from equation (1) and from equations (4) and (5), respectively.

They are the same as those of the FeSi/Si CMF with different FeSi layer thicknesses [1], and close to those obtained from Fe<sub>50</sub>Si<sub>50</sub> amorphous films reported by Oswald *et al* [7]. This indicates that for the FeSi/Si CMF with different FeSi or Si layer thicknesses, the Fe atoms in the dead layers are in the same chemical circumstances and geometric structures which are similar to those in the amorphous Fe<sub>50</sub>Si<sub>50</sub> films.

Figure 2 shows the hyperfine fields  $H_f$  of samples and the thickness  $d_p$  of the dead layers as functions of the thickness  $d_s$  of the Si layers. When the Si layers are thicker than 30 Å, the values of  $H_f$  and  $d_p$  change slightly with varying  $d_s$ . When  $d_s$  becomes smaller than 30 Å, the thickness of the dead layers decreases rapidly and the hyperfine field of the samples increases rapidly. When  $d_s$  is reduced to a certain value, the thickness of the dead layers decreases to zero. This indicates that there is a coupling between the magnetic layers when the Si layers are thin enough. This coupling includes the dipolar and exchange interactions of magnetization in the magnetic layers through the barrier of the Si layers, and the exchange interaction of magnetic moments of the Fe atoms in the interfaces through the Fe atoms which are inevitably introduced into the Si layers by the sputtering process. Because of the atomic interdiffusion of interlayers which mainly came from the ion implantation effect during the sputtering process, a dead layer which consists of the paramagnetic clusters of iron atoms and a weak magnetic transitional layer with a lower concentration of iron atoms would be formed at the interface. When the Si layers are thick enough, the coupling between FeSi layers is very weak and even isolated, the magnetic properties of samples are mainly determined by the individual FeSi layers. When the Si layers are thin enough, the coupling between the magnetic layers strengthens rapidly. This results in a decrease in the number of paramagnetic iron atoms in the dead layers, and enhancement of the magnetic moments of iron atoms in the weak magnetic transitional layers. Therefore, the thickness of the dead layers decreases and the hyperfine field of the samples increases.

The dependence of the thickness  $d_p$  of the dead layers on the Si layer thickness  $d_s$  is assumed to be the following relation:

$$d_p = d_p(\infty)\{1 - \exp[-\beta(d_s - t)]\} \quad (1)$$

where  $d_p(\infty)$  is the thickness of the dead layers with  $d_s \rightarrow \infty$ , and  $t$  is the thickness of the Si layers at which  $d_p = 0$ .  $\beta$  is a coefficient which determines the decreasing rate of the thickness of the dead layers with decreasing thickness of the Si layers. Equation (1) indicates that the iron atoms introduced into the Si layers by the sputtering process are in an exponential distribution with respect to depth into the Si layers. The experimental

data of  $d_p$  are fitted by using equation (1). The result of the fitting is shown by the full curve of  $d_p$  in figure 2, where  $d_p(\infty) = 3.1 \text{ \AA}$ ,  $t = 5 \text{ \AA}$  and  $\beta = 0.13 \text{ \AA}^{-1}$ . This means that, when the thickness of the Si layers is reduced to  $5 \text{ \AA}$ , the iron atoms diffused into the Si layers from the FeSi layers on both sides of Si layers superpose so seriously that the number of paramagnetic iron atoms in the dead layers decreases to zero, and the dead layers disappear accordingly.

The hyperfine fields of the FeSi/Si CMF can be expressed as follows [1]:

$$H_f = H_f(\infty)[1 - d'_D/(d_m - d_p)] \quad (2)$$

where  $H_f(\infty)$  is the hyperfine field of amorphous  $\text{Fe}_{80.5}\text{Si}_{19.5}$  bulk alloy,  $d_m$  is the thickness of the FeSi layers (in our case,  $d_m = 17 \text{ \AA}$ ),  $d_p$  is the thickness of the dead layers for the FeSi/Si CMF with the Si layers thickness of  $d_s$ .  $d'_D$  is the thickness of the effective 'dead layer' which originated as follows. The weak magnetic transitional layers in the interfaces can be divided into two parts: one with the same hyperfine field as that in the interior of the FeSi layers and the other with a zero hyperfine field which is defined as the effective 'dead layer'. Since the CEMS measurements were performed at room temperature, the value of  $d'_D$  would include the contribution of the dimensional effect [1]. It is easy to infer that, only when the thickness of the Si layers is reduced to zero, will the value of  $d'_D$  be zero and the value of  $H_f$  will reach the maximum which corresponds to the hyperfine field of amorphous FeSi bulk alloy. Assume that the relation between  $d'_D$  and  $d_s$  satisfies equation (1), i.e.

$$d'_D = d'_D(\infty)[1 - \exp(-\beta'd_s)] \quad (3)$$

where  $d'_D(\infty)$  is the thickness of the effective 'dead layer' when  $d_s \rightarrow \infty$ . Substituting equations (1) and (3) into equation (2), the dependence of  $H_f$  on  $d_s$  can be obtained as follows:

$$H_f = H_f(\infty) \left( 1 - \frac{d'_D(\infty)[1 - \exp(-\beta'd_s)]}{\|d_m - d_p(\infty)\{1 - \exp[-\beta(d_s - t)]\}\|} \right) \quad \text{for } d_s > t \quad (4)$$

and

$$H_f = H_f(\infty)\{1 - [d'_D(\infty)/d_m][1 - \exp(-\beta'd_s)]\} \quad \text{for } d_s \leq t. \quad (5)$$

Here  $H_f(\infty) = 302.4 \text{ kOe}$  was obtained from the CEMS experiment on the FeSi/Si CMF with different FeSi layer thicknesses [1];  $d_m = 17 \text{ \AA}$ ,  $d_p(\infty) = 3.1 \text{ \AA}$ ,  $t = 5 \text{ \AA}$  and  $\beta = 0.13 \text{ \AA}^{-1}$ . A fit to the experimental data has been made by using equations (4) and (5). The result is shown in figure 2 by the full curve of  $H_f$ , where  $d'_D(\infty) = 5.1 \text{ \AA}$ , and  $\beta' = 0.18 \text{ \AA}^{-1}$ . As shown in figure 2, the theoretical curve is in good agreement with the experimental data. This indicates that equations (4) and (5) describe appropriately the dependence of the hyperfine fields of samples on the thickness of the Si layers.

In the Mössbauer spectra with six lines, the relative peak intensity of the second or fifth line reflects the angle between the direction of the hyperfine field and  $\gamma$ -rays. We can see from figure 1(b) that, for the sample with Si layers as thin as  $8.8 \text{ \AA}$ , the peak intensity of the second or fifth line in the Mössbauer spectrum is much lower than others but, for other samples with thicker Si layers, the peak intensity of the second or fifth line is higher than that of the first or sixth line as shown in figure 1. In order to identify this difference, we inspected the magnetic properties of various samples with different Si layer thicknesses and found that the sample with Si layers as thin as  $8.8 \text{ \AA}$  has a perpendicular anisotropy as large as  $3 \times 10^4 \text{ A m}^{-1}$  (about  $400 \text{ Oe}$ ) (measured by the

hysteresis loop and the magnetic torque), but the others do not have this anisotropy or only have a very small anisotropy. This indicates that the difference between the relative peak intensities of Mössbauer spectra is caused by the difference between the magnetization directions of the samples with respect to the  $\gamma$ -ray direction. For the sample with Si layers as thin as 8.8 Å, the direction of magnetization is out of the film plane, but for the others it is in the film plane. The origin of this perpendicular anisotropy is not clear yet. It seems different from the surface (or interface) anisotropy proposed by Néel [8] and Gradmann [9] and is probably related to the coupling of interlayers.

#### 4. Conclusions

The CEMS study on amorphous FeSi/Si CMFs showed that the coupling between the magnetic layers strengthened with decreasing Si layer thickness. This results in decreasing thickness of the dead layers at the interfaces and increasing hyperfine fields of FeSi/Si CMFs. The thickness of the dead layers decreases exponentially with decreasing Si layer thickness. When the thickness of the Si layer is reduced to 5 Å, the dead layers disappear. When the Si layers are thinner than 8.8 Å, the direction of the magnetization is out of the film plane.

#### Acknowledgments

The authors would like to thank J S Lan and M Li for help with the experiments. This work was supported by the National Natural Science Foundation of China.

#### References

- [1] Ma X D, Liu Y H and Mei L M 1991 *J. Magn. Magn. Mater.* **95** 199
- [2] Liu Y H, Ma X D and Mei L M 1990 *Acta Phys. Sin.* **39** 2005 (in Chinese)
- [3] Shinjo T, Hosoi H, Kawaguchi K, Nakayama N, Takada T and Endoh Y 1986 *J. Magn. Magn. Mater.* **54–57** 737
- [4] Liu Y H and Yang L Q 1988 *J. Magn. Magn. Mater.* **75** 263
- [5] Shimada Y and Kojima H 1976 *J. Appl. Phys.* **47** 4156
- [6] Meisel W 1971 *Exp. Tech. Phys.* **19** 23
- [7] Oswald R S, Ron M and Ohring M 1978 *Solid State Commun.* **26** 883
- [8] Néel L 1953 *C. R. Acad. Sci., Paris* **237** 1468
- [9] Gradmann U 1974 *Appl. Phys.* **3** 161